

# Stable isotopic analysis of atmospheric methane by infrared spectroscopy by use of diode laser difference-frequency generation

Michael E. Trudeau, Pin Chen, Guilherme de Andrade Garcia, Leo W. Hollberg, and Pieter P. Tans

An infrared absorption spectrometer has been constructed to measure the stable isotopic composition of atmospheric methane samples. The spectrometer employs periodically poled lithium niobate to generate 15  $\mu\text{W}$  of tunable difference-frequency radiation from two near-infrared diode lasers that probe the  $\nu_3$  rotational-vibrational band of methane at 3.4  $\mu\text{m}$ . To enhance the signal, methane is extracted from 25 l of air by use of a cryogenic chromatographic column and is expanded into the multipass cell for analysis. A measurement precision of 12‰ is demonstrated for both  $\delta^{13}\text{C}$  and  $\delta\text{D}$ . © 2006 Optical Society of America

OCIS codes: 010.1280, 300.6420.

## 1. Introduction

Methane is an important radiative trace gas that has contributed an estimated  $0.48 \text{ W/m}^2$  to the change in the radiative balance of the atmosphere, corresponding to approximately 20% of the total increase during the past century.<sup>1</sup> The current globally averaged atmospheric surface methane mixing ratio of  $\sim 1745$  parts in  $10^9$  (ppb) is more than double preindustrial estimates, an increase that has largely been attributed to human activities.<sup>2</sup> Legislative regulation and abatement strategies to control future concentrations of atmospheric methane require identifying and assessing methane source and sink magnitudes.

Precise measurements of mixing ratios and isotopic compositions of atmospheric background samples add constraints to global methane models that help resolve uncertainties in the sources and sinks. To date, isotopic measurements of atmospheric methane samples have been performed almost exclusively by isotope ratio mass spectrometry (see, for instance, Quay *et al.*<sup>3</sup> and Kuhlmann *et al.*<sup>4</sup>). Measurements of  $^{13}\text{C}$  and  $^2\text{H}$  in methane by conventional mass spectrometry require procedures to convert  $\text{CH}_4$  to  $\text{CO}_2$  and  $\text{H}_2\text{O}$  (followed by the reduction of  $\text{H}_2\text{O}$  to  $\text{H}_2$ ) since  $^{13}\text{CH}_4$  and  $^{12}\text{CH}_3\text{D}$  share a small mass difference of 0.003 amu that is below instrument mass resolution. More recent reports of high-precision continuous-flow measurements using pyrolysis to convert  $\text{CH}_4$  directly to  $\text{H}_2$  have been made.<sup>5</sup> However, optical analysis of isotopic composition allows simultaneous measurement of both carbon and deuterium isotopes in methane without chemical conversion and minimizes possible interference by other hydrocarbons. Moreover, optical analysis allows for compact and energy-efficient spectrometers to be constructed with diode lasers, facilitating field measurements.

Several reports of the use of infrared laser spectroscopy to measure methane isotopic composition exist in the literature. Kosterev *et al.*<sup>6</sup> reported measurements of isotopic composition with a quantum-cascade laser that probes the  $\nu_4 P$  branch of methane at 8.1  $\mu\text{m}$  (no measurement uncertainty

---

M. E. Trudeau (michael.trudeau@noaa.gov) is with the Earth System Research Laboratory, National Oceanic and Atmospheric Administration, P.O. Box 275, Hilo, Hawaii 96720. P. Chen is with the Jet Propulsion Laboratory, 4800 Oak Grove Drive, Pasadena, California 91109. G. A. Garcia is with the Instituto Nacional de Metrologia, Normalizacao e Qualidade Industrial, Avenida Nossa Senhora das Gracas 50, Predio 3, Xerem Duque de Caxias, Rio de Janeiro 25250-020, Brazil. L. W. Hollberg is with the Time and Frequency Division, National Institute of Standards and Technology, 325 Broadway, Boulder, Colorado 80305. P. P. Tans is with the Earth System Research Laboratory, National Oceanic and Atmospheric Administration, 325 Broadway, Boulder, Colorado 80305.

Received 14 October 2005; revised 25 January 2006; accepted 26 January 2006; posted 26 January 2006 (Doc. ID 65310).

0003-6935/06/174136-06\$15.00/0

© 2006 Optical Society of America

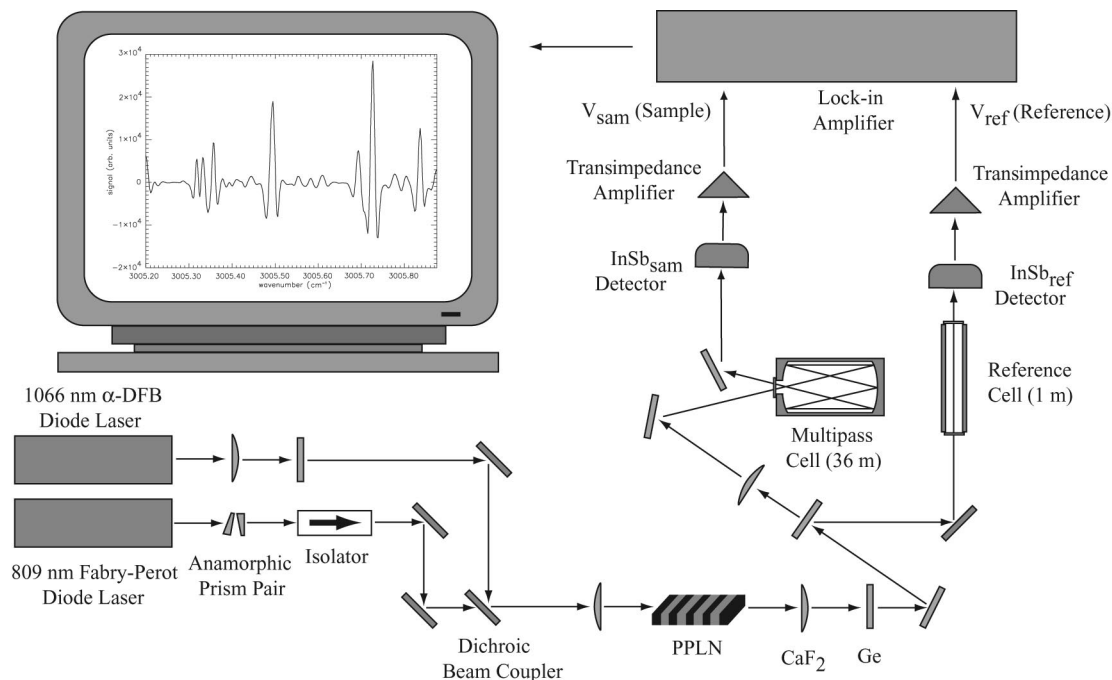


Fig. 1. Optical design of the laser spectrometer shown with a typical spectrum.

was reported). Dahnke *et al.*<sup>7</sup> reported a  $\delta^{13}\text{C}$  precision of  $\pm 11\%$  (parts per thousand) on ambient air samples by use of cavity leak-out spectroscopy in the  $3\ \mu\text{m}$  wavelength region. Yamamoto and Yoshida<sup>8</sup> demonstrated the use of the methane overtone transition, in the  $1.7\ \mu\text{m}$  spectral region, to probe pure methane samples with a precision of  $\pm 0.7\%$  and  $\pm 0.027\%$  for  $\delta^{13}\text{C}$  and  $\delta\text{D}$ , respectively. Bergamaschi *et al.*<sup>9</sup> described a liquid-nitrogen-cooled lead salt tunable diode laser absorption spectrometer for isotope measurements of methane sources, and in a more recent publication<sup>10</sup> reported an uncertainty of  $\pm 0.5$  to  $\pm 1.0\%$  for  $^{12}\text{CH}_3\text{D}/^{12}\text{CH}_4$  measurements at  $\sim 3.3\ \mu\text{m}$  on pre-concentrated samples of background air. Measurements of unprocessed ambient methane mixing ratios have been made by Petrov *et al.*<sup>11</sup> with an uncertainty of  $< 1$  ppb using difference-frequency generation (DFG) in periodically poled lithium niobate (PPLN), and Waltman *et al.*<sup>12</sup> reported measurements of  $^{13}\text{CH}_4/^{12}\text{CH}_4$  isotopic ratios using the same technique with an uncertainty of  $\pm 44\%$ . Although this is insufficient for routine monitoring of methane isotopic ratios of background atmospheric methane, the technique employs commercial near-infrared diode lasers, which offer the potential for single-frequency operation at temperatures that can be reached with Peltier coolers. The present work extends DFG and sample pre-concentration to measurements of both methane  $^{13}\text{C}/^{12}\text{C}$  and deuterium/hydrogen (D/H) ratios.

Here we present the results of two sets of experiments in the  $3.32\text{--}3.41\ \mu\text{m}$  ( $3020\text{--}2930\ \text{cm}^{-1}$ ) spectral region. The first set of experiments determined the hydrogen isotopic composition of methane with measurements of the  $2950.8508/2951.3057\ \text{cm}^{-1}$

( $^{12}\text{CH}_3\text{D}/^{12}\text{CH}_4$ ) line pair. A second set of experiments used the  $3005.3149/3005.7333\ \text{cm}^{-1}$  ( $^{13}\text{CH}_4/^{12}\text{CH}_4$ ) line pair for carbon isotope measurements. The HITRAN atmospheric molecular spectroscopy database (Methane Update v11.0) was used to identify line pairs in both spectral regions. Absorption line pairs were used to calculate the measurement uncertainty in methane isotopic signatures and demonstrate the application of this technique to background monitoring of atmospheric methane isotope variability.

## 2. Instrument Design

The instrument design for the laser spectrometer is shown in Fig. 1. The optical configuration for the DFG absorption spectrometer consists of a 100 mW AlGaAs Fabry-Perot diode laser at 809 nm (pump) and a 500 mW distributed-feedback ( $\alpha$ -DFB) diode laser at 1066 nm (signal). The laser outputs are combined by a dichroic beam coupler and focused into a temperature-tunable, quasi-phase-matched nonlinear  $\text{LiNO}_3$  crystal with a  $22.2\ \mu\text{m}$  domain period. The crystal has a conversion efficiency of  $0.4\ \text{mW W}^{-2}\ \text{cm}^{-1}$ , 60% of the theoretical value. The resulting  $\sim 3.3\ \mu\text{m}$  radiation (idler) is passed through a germanium filter with a net power of  $\sim 15\ \mu\text{W}$ . The optical configuration for experiments in the  $3005\ \text{cm}^{-1}$  spectral region includes a zinc selenide beam splitter that divides the transmitted beam. One beam is focused onto a  $300\ \text{cm}^3$  multipass absorption cell with a path length of 36 m and the second beam is focused onto a  $500\ \text{cm}^3$  single-pass reference cell (1.0 m in length). The reference cell is filled with a gas that is 0.1810% (by mole fraction)  $\text{CH}_4$  in ambient mixing ratios of  $\text{N}_2$ ,  $\text{O}_2$ , and

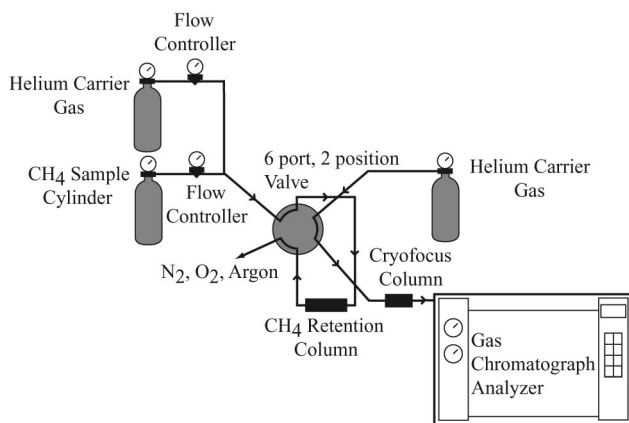


Fig. 2. Cryogenic methane trap diagram.

argon. The reference cell gas pressure is set to match the full width at half-maximum of the reference absorption peak to that of the sample peak. Experiments in the  $2950\text{ cm}^{-1}$  spectral region were performed prior to the addition of the reference cell to the instrument design and therefore do not include reference gas measurements. Optical throughput of the multipass cell is 17%. The beams from each absorption cell are directed onto InSb photodiode infrared detectors cooled by liquid nitrogen with a background-limited noise-equivalent power of  $\sim 2 \times 10^{-12}\text{ W Hz}^{-1/2}$ . Wavelength modulation of the pump laser at  $\sim 2\text{ kHz}$  with a modulation depth of  $\sim 0.02\text{ cm}^{-1}$  was utilized to reduce spectrometer noise while the idler frequency was scanned over the selected spectral regions of  $\sim 1.0\text{ cm}^{-1}$  at  $10\text{ Hz}$  by tuning the current of the signal laser. For the experiments in the  $2950\text{ cm}^{-1}$  spectral region we used a solenoid to mechanically vibrate the multipass cell to average out deleterious interference fringes. The detector signal was processed with a lock-in amplifier, and the second-harmonic signal from the wavelength modulation was used for isotopic ratio calculations. Each spectrum is an average of 1000 scans.

A cylinder of air filled at an altitude of 3523 m at Niwot Ridge, Colorado, was used as the sample gas for experiments in both spectral regions and was measured to be 1763 ppb methane by the National Oceanic and Atmospheric Administration's Earth System Research Laboratory Carbon Cycle Greenhouse Gases Group. This cylinder should reflect the methane isotopic signature of clean background air and so was not calibrated for isotopes. Given the noise-equivalent power, a noise-equivalent bandwidth of 0.78 Hz, the cylinder methane mixing ratio, and spectroscopic values listed in the HITRAN database, the estimated signal-to-noise ratio at the sample cell detector (InSb<sub>sam</sub> in Fig. 1) is  $\sim 16$  for the weakest absorption line at  $2950.8508\text{ cm}^{-1}$ . For application to atmospheric monitoring of background methane isotopic ratios, the target instrument uncertainty should be 1 part per thousand. To enhance the signal-to-noise ratio, preconcentration proce-

dures are implemented to increase methane partial pressures.

The design for methane cryogenic enrichment is shown in Fig. 2. Methane was extracted from 25 l of air for isotopic measurements of the  $^{13}\text{C}/^{12}\text{C}$  line pair. The sample air is passed through a 3/8 in. (0.95 cm) stainless-steel chromatographic column packed with a 2 g 80/100 carbon molecular sieve and a sheathed resistance temperature detector sensor (see Retention Column in Fig. 2). The column is contained in an elliptical cavity with a 150 W halogen filament and liquid-nitrogen inlet to control temperature cycling and is initially baked out at  $300\text{ }^\circ\text{C}$  for 30 min under a 30 ml/min dry helium flow before sample introduction. The temperature is then decreased to  $-180\text{ }^\circ\text{C}$  for 30 min, after which the air sample is passed at a flow rate of 200 ml/min at  $25\text{ }^\circ\text{C}$  and 1 atm. Following sample concentration on the chromatographic column, the helium flow is reinitiated and a temperature ramp begins that increases the column temperature to  $-155\text{ }^\circ\text{C}$  at a rate of  $1\text{ }^\circ\text{C}/\text{min}$ . Solenoid valves then isolate the column, the temperature is increased to  $300\text{ }^\circ\text{C}$ , and the sample is passed under a helium flow to a portable cryofocus column containing 1.0 g of carbon molecular sieve in a liquid-nitrogen bath. The cryofocus column is removed from the liquid nitrogen, allowed to reach room temperature, and the methane sample is expanded into the evacuated multipass cell for isotopic analysis. The total time for preconcentration is  $\sim 4\text{ h}$ . The extraction procedure produces a methane mole fraction of 0.448% ( $4.48\text{ mmol mol}^{-1}$ ) at a total pressure of 27 Torr in the multipass cell, corresponding to a mole fraction enrichment of 2540 times. Measurements of the D/H line pair used 20 l of air for the extraction process and did not implement the temperature ramp at the end of the preconcentration procedure. This extraction resulted in a multipass cell methane mole fraction of 0.102% ( $1.02\text{ mmol mol}^{-1}$ ) at a pressure of 95 Torr, an enrichment of 578 times relative to the methane mixing ratio of the cylinder. Trapping efficiency increased with the addition of the temperature ramp to the carbon isotopic ratio measurements, a process that desorbs excess  $\text{O}_2$  and  $\text{N}_2$  from the column that would otherwise contribute to pressure broadening of the absorption lines. The balance of gas contribution to the cell pressure comes largely from  $\text{CO}_2$  that is retained during the extraction process. The air leaving the cryogenic apparatus for experiments in both spectral regions was continuously sampled for methane by a gas chromatograph analyzer with a measurement uncertainty of  $\sim 7\text{ ppb}$ , quantitatively retaining methane to  $\pm 0.4\%$ .

These experiments did not include an investigation of possible isotope fractionation during preconcentration. All uncertainties presented in this paper refer to measurements of single samples. Isotope fractionation in the preconcentration procedure, the expansion of the methane sample into the absorption cell following preconcentration, as well as other steps in the measurement process require a study of long-

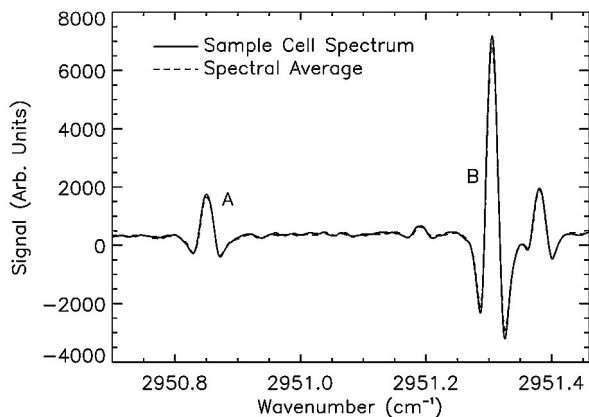


Fig. 3. Second-harmonic signal of methane in the D/H spectral region. The sample gas spectrum is shown as the solid curve, overlaid with the spectral average of all sample gas scans (dashed curve) used as the reference spectrum. The deuterium absorption is labeled as peak A and hydrogen as peak B.

term measurement reproducibility and systematic errors in isotope signature assignments with calibrated isotope standards.

### 3. Data Analysis and Discussion

Ten spectra of the D/H line pair were recorded on a single preconcentrated sample. A single spectrum and the spectral average are shown in Fig. 3. For measurements of the carbon isotopic ratio using the 3005.3149/3005.7333  $\text{cm}^{-1}$  line pair, two different preconcentrated samples were analyzed on each of two days with simultaneous reference gas measurements. Ten spectra were recorded sequentially of each preconcentrated sample. Background spectra of the evacuated multipass cell before analysis were then subtracted from the absorption spectra to remove the contribution of residual water vapor in the multipass cell at 3005.44  $\text{cm}^{-1}$ . Figure 4 shows a sample cell spectrum and reference cell spectrum of the carbon isotope line pair. All spectra are corrected for a nonlinear response in laser wavelength to fast current tuning of the diode lasers.

Spectral lines were chosen to match absorption signal intensities by pairing a strong transition of the rare isotope to a weak transition of the abundant isotope. The difference in ground-state energies between line pairs results in a temperature dependence in the relative population of states and a temperature sensitivity in isotopic signature assignments. The estimated temperature dependences for the  $^{13}\text{CH}_4/^{12}\text{CH}_4$  and  $^{12}\text{CH}_3\text{D}/^{12}\text{CH}_4$  line pairs are 23.1 and 5.1%/K, respectively, calculated using the relationship of Bergamaschi *et al.*<sup>9</sup> and ground-state energies from the HITRAN database. Although not implemented in this study, corrections to the isotopic signature assignments for temperature variations between sample and reference cells can be made with zero measurements as described by Bergamaschi *et al.*<sup>9</sup>

Table 1 summarizes the significant isotopic contri-

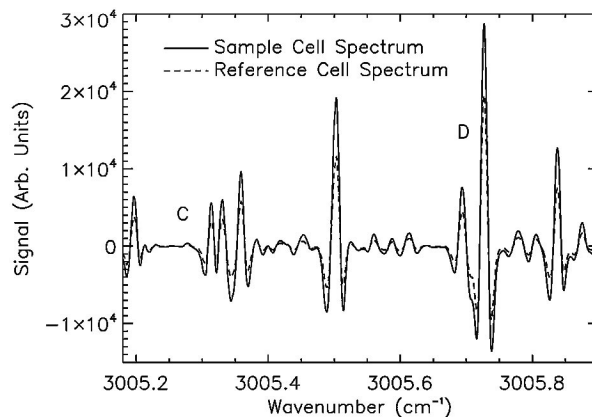


Fig. 4. Second-harmonic signal of methane in the  $^{13}\text{C}/^{12}\text{C}$  spectral region. The sample cell spectrum is shown as the solid curve and the corresponding reference spectrum as the dashed curve.  $^{13}\text{C}$  absorption is labeled as peak C and  $^{12}\text{C}$  as peak D.

butions to the observed line profiles shown in Figs. 3 and 4. Spectral resolution was limited by an absorption linewidth of approximately 0.02  $\text{cm}^{-1}$ , due to a combination of pressure and Doppler broadening. The 2950.8508/2951.3057  $\text{cm}^{-1}$  line pair of the  $\nu_3$  P branch, labeled as line profiles A and B in Fig. 3, is used for the D/H isotopic ratio calculations. Peak A is an absorption feature of  $^{12}\text{CH}_3\text{D}$  at 2950.8508  $\text{cm}^{-1}$  with underlying  $^{12}\text{CH}_4$  absorption at 2950.8627  $\text{cm}^{-1}$  that contributes approximately 5.0% to the total line intensity. Peak B is a  $^{12}\text{CH}_4$  isotopic line at 2951.3057  $\text{cm}^{-1}$  with neighboring  $^{12}\text{CH}_4$  absorption at 2951.3816  $\text{cm}^{-1}$  and an underlying contribution of 1.5% from  $^{12}\text{CH}_3\text{D}$  absorption at 2951.3598  $\text{cm}^{-1}$ . The convolution of isotopic line profiles with those of other species requires simultaneous measurements of pure isotopic calibration gases for isotopic signature assignments. For estimates of the D/H measurement precision, underlying absorption by neighboring isotopes is relatively small and has been neglected.

The 3005.3149/3005.7333  $\text{cm}^{-1}$  line pair (labeled as C and D in Fig. 4) of the  $\nu_3$  Q branch was used to calculate the  $^{13}\text{C}/^{12}\text{C}$  ratio. Absorption peak C is a  $^{13}\text{CH}_4$  isotopic peak at 3005.3149  $\text{cm}^{-1}$  with a neighboring  $^{13}\text{CH}_4$  absorption feature at 3005.3305  $\text{cm}^{-1}$  and underlying absorption from  $^{12}\text{CH}_4$  at 3005.3011  $\text{cm}^{-1}$ . Using HITRAN line intensities,  $^{12}\text{CH}_4$  contributes 0.6% to the total line profile and is comparable to the measurement uncertainty. Peak D is pure isotopic absorption by  $^{12}\text{CH}_4$  at 3005.7333  $\text{cm}^{-1}$  and has adjacent absorption features of the same isotope centered at 3005.6951 and 3005.7266  $\text{cm}^{-1}$ . The spectral region containing peaks C and D was chosen following the first experiments (in the 2950  $\text{cm}^{-1}$  spectral region) for an intense deuterium transition, according to the HITRAN 2000 database. With the methane update in 2001, this absorption feature was reassigned to the  $^{13}\text{CH}_4$  and  $^{12}\text{CH}_4$  isotopes. This demonstrates the importance of independent measurements of the isotopic lines of interest.

Singular-value decomposition was used to calcu-

**Table 1. Estimated Line Intensity Contributions of Methane Isotopes (HITRAN) to the Observed Absorption Profiles<sup>a</sup>**

| Absorption Profile Identification                            | A                         | B                         | C                         | D                         |
|--|---------------------------|---------------------------|---------------------------|---------------------------|
| <sup>12</sup> CH <sub>4</sub>                                |                           |                           |                           |                           |
| Wavenumber (cm <sup>-1</sup> )                               | 2950.8627                 | 2951.3057                 | 3005.3011                 | 3005.7333                 |
| Line intensity, S [cm <sup>-1</sup> (mol cm <sup>-2</sup> )] | 1.447 × 10 <sup>-24</sup> | 1.241 × 10 <sup>-22</sup> | 1.467 × 10 <sup>-24</sup> | 3.041 × 10 <sup>-23</sup> |
| Relative contribution (%)                                    | 5                         | 98.5                      | 0.6                       | 100                       |
| <sup>13</sup> CH <sub>4</sub>                                |                           |                           |                           |                           |
| Wavenumber (cm <sup>-1</sup> )                               | —                         | —                         | 3005.3149                 | —                         |
| Line intensity, S [cm <sup>-1</sup> (mol cm <sup>-2</sup> )] | —                         | —                         | 2.478 × 10 <sup>-22</sup> | —                         |
| Relative contribution (%)                                    | —                         | —                         | 99.4                      | —                         |
| <sup>12</sup> CH <sub>3</sub> D                              |                           |                           |                           |                           |
| Wavenumber (cm <sup>-1</sup> )                               | 2950.8508                 | 2951.3598                 | —                         | —                         |
| Line intensity, S [cm <sup>-1</sup> (mol cm <sup>-2</sup> )] | 2.73 × 10 <sup>-23</sup>  | 1.884 × 10 <sup>-24</sup> | —                         | —                         |
| Relative contribution (%)                                    | 95                        | 1.5                       | —                         | —                         |

<sup>a</sup>Peaks A–D in Figs. 3 and 4.

late the relative contributions of each reference isotopic peak to the sample spectra. The isotopic composition of each spectrum is expressed as the relative difference in absorption intensities between sample and reference gases in conventional per thousand notation, according to Eq. (1):

$$\delta(^{13}\text{C or D}) = (R_{\text{sam}}/R_{\text{ref}} - 1) \times 1000. \quad (1)$$

The isotopic ratio  $R$  is the ratio of the concentration of the rare to abundant isotope and represents the ratio of peak intensities for D/H ( $[A]/[B]$ ) and <sup>13</sup>C/<sup>12</sup>C ( $[C]/[D]$ ), where absorption intensities (e.g.,  $[A]$ ) are the singular-value decomposition coefficients of their respective peaks. For the intercomparison of isotopic measurements between laboratories, reference gas measurements require independent isotopic signature assignments on the internationally recognized PeeDee Belemnite (PDB) and Vienna Standard Mean Ocean Water (V-SMOW) measurement scales for <sup>13</sup>C and <sup>2</sup>H, respectively.<sup>13</sup> These signature assignments are unnecessary for measurement precision calculations and are not made for these experiments.

Table 2 summarizes measurement precision calculations for experiments in both spectral regions. The reported precision is one standard deviation of the isotopic signature in units of per thousand. Since measurements of the D/H line pair were performed without the reference cell, the average of all sample cell spectra, referred to as  $R_{\text{ave,sam}}$  in Table 2, was used

in place of the reference cell spectra ( $R_{\text{ref}}$ ) in precision calculations. The same procedure was used with both sample and reference cell spectra of the <sup>13</sup>C/<sup>12</sup>C line pair for comparison. The precision for  $\delta\text{D}$  was  $\pm 12\%$  using the spectral average as the reference spectrum. Sample cell precision was  $\pm 38\%$  and  $\pm 69\%$  for  $\delta^{13}\text{C}$  for the first and second days of analysis, respectively. Reference cell precision was within a few per thousand of the sample cell on each of the two days. When experimentally measured reference spectra are used in the calculation for  $\delta^{13}\text{C}$ , the uncertainty improves to  $\pm 10\%$  and  $\pm 13\%$  on the first and second days of analysis, respectively. The significant improvement in measurement uncertainty demonstrates the value of simultaneously measured reference spectra as a means to correct for variations in instrument response.

Given equivalent experimental conditions for measurements in both spectral regions, the ninefold difference in isotopic line strengths (3005.3149/2950.8508 cm<sup>-1</sup> line pair) could be expected to translate into a similar improvement in  $\delta^{13}\text{C}$  measurement uncertainty. However, an important difference in instrument configuration between measurements in each spectral region was the mechanical vibration of the multipass cell. Spectral shifts of the interference fringe pattern with mechanical vibration of the multipass cell reduce the fringe amplitude with spectral averaging and create a stable baseline structure. The spectra used for the  $\delta^{13}\text{C}$  calculations were recorded without this technique and therefore contain a larger interference fringe component that results in a lower than expected measurement uncertainty. The  $\delta\text{D}$  analysis shows comparable precision to the  $\delta^{13}\text{C}$  analysis due to mechanical jittering of the sample cell even though the intrinsic line strength for deuterium is much weaker and no reference cell was used in the experimental setup. Additional measurement uncertainty may have also been introduced through the use of epoxy to seal small leaks in the vacuum system for this instrument. Sample gas contact with polymeric materials, such as plastics and adhesives, has been observed to systematically affect trace gas measure-

**Table 2. Measurement Uncertainty Summary**

| Experiment (cm <sup>-1</sup> ) | Spectral Ratio                      | Uncertainty, % ( $\pm 1\sigma$ ) |
|--------------------------------|-------------------------------------|----------------------------------|
| 2950                           | $R_{\text{sam}}/R_{\text{ave,sam}}$ | 12                               |
| 3005, day 1                    | $R_{\text{sam}}/R_{\text{ave,sam}}$ | 38                               |
| 3005, day 1                    | $R_{\text{ref}}/R_{\text{ave,ref}}$ | 42                               |
| 3005, day 2                    | $R_{\text{sam}}/R_{\text{ave,sam}}$ | 69                               |
| 3005, day 2                    | $R_{\text{ref}}/R_{\text{ave,ref}}$ | 67                               |
| 3005, day 1                    | $R_{\text{sam}}/R_{\text{ref}}$     | 10                               |
| 3005, day 2                    | $R_{\text{sam}}/R_{\text{ref}}$     | 13                               |

ments of carbon monoxide and carbon dioxide,<sup>14</sup> and an effect on methane isotope measurements cannot be dismissed as a contributing source of error without further study.

#### 4. Conclusions

In this analysis, DFG in PPLN using near-infrared diode lasers was tested in the construction of a laser spectrometer for measurements in the 3000 cm<sup>-1</sup> region of methane <sup>13</sup>C/<sup>12</sup>C and D/H isotopic ratios. Experiments were done with actual air samples at levels typical of background atmospheric mixing ratios. We demonstrated that this technique could be used with a measurement uncertainty for pre-concentrated atmospheric methane samples of a few parts per hundred. For the application of this instrument to atmospheric monitoring of methane isotopic ratios, calibration standards would be required to assign isotopic signatures on the international PDB and V-SMOW isotopic scales for <sup>13</sup>C and <sup>2</sup>H.

The authors are grateful to the Environmental Protection Agency (STAR Fellowship); the National Research Council (Postdoctoral Research Associateship Program); and the Fundação de Amparo a Pesquisa do Estado de São Paulo, Brazil, for financial support of this work. The authors thank E. Dlugokencky at the National Oceanic and Atmospheric Administration's Earth System Research Laboratory for providing calibrated ambient air samples.

#### References

1. V. Ramaswamy, O. Boucher, J. Haigh, D. Hauglustaine, J. Haywood, G. Myhre, T. Nakajima, G. Y. Shi, and S. Solomon, "Radiative forcing of climate change," in *Climate Change 2001: The Scientific Basis. Contribution of Working Group I to the Third Assessment Report of the Intergovernmental Panel on Climate Change*, J. T. Houghton, Y. Ding, D. J. Griggs, M. Noguer, P. J. van der Linden, X. Dai, K. Maskell, and C. A. Johnson, eds. (Cambridge U. Press, 2001), pp. 349–416.
2. M. A. K. Khalil and R. A. Rasmussen, "Atmospheric methane: trends over the last 10,000 years," *Atmos. Environ.* **21**, 2445–2452 (1987).
3. P. Quay, J. Stutsman, D. Wilbur, A. Snover, E. Dlugokencky, and T. Brown, "The isotopic composition of atmospheric methane," *Global Biogeochem. Cycles* **13**, 445–461 (1999).
4. A. J. Kuhlmann, D. E. J. Worthy, N. B. A. Trivett, and I. Levin, "Methane emissions from a wetland region within the Hudson Bay Lowland: an atmospheric approach," *J. Geophys. Res.* **103D**, 16009–16016 (1998).
5. A. L. Rice, A. A. Gotoh, H. O. Ajie, and S. C. Tyler, "High-precision continuous-flow measurement of delta C-13 and delta D of atmospheric CH<sub>4</sub>," *Anal. Chem.* **73**, 4104–4110 (2001).
6. A. A. Kosterev, R. F. Curl, F. K. Tittel, C. Gmachl, F. Capasso, D. L. Sivco, J. N. Baillargeon, A. L. Hutchinson, and A. Y. Cho, "Methane concentration and isotopic composition measurements with a mid-infrared quantum cascade laser," *Opt. Lett.* **24**, 1762–1764 (1999).
7. H. Dahnke, D. Kleine, W. Urban, P. Hering, and M. Murtz, "Isotopic ratio measurements of methane in ambient air using mid-infrared cavity leak-out spectroscopy," *Appl. Phys. B* **72**, 121–125 (2001).
8. K. Yamamoto and N. Yoshida, "High-precision isotopic ratio measurement system for methane (<sup>12</sup>CH<sub>3</sub>D/<sup>12</sup>CH<sub>4</sub>, <sup>13</sup>CH<sub>4</sub>/<sup>12</sup>CH<sub>4</sub>) by using near-infrared diode laser absorption spectroscopy," *Spectrochim. Acta Part A* **58**, 2699–2707 (2002).
9. P. Bergamaschi, M. Schupp, and G. W. Harris, "High-precision direct measurements of <sup>13</sup>CH<sub>4</sub>/<sup>12</sup>CH<sub>4</sub> and <sup>12</sup>CH<sub>3</sub>D/<sup>12</sup>CH<sub>4</sub> ratios in atmospheric methane sources by means of a long-path tunable diode laser absorption spectrometer," *Appl. Opt.* **33**, 7704–7716 (1994).
10. P. Bergamaschi, M. Bräunlich, T. Marik, and C. Brenninkmeijer, "Measurements of carbon and hydrogen isotopes of atmospheric methane at Izaña, Tenerife: seasonal cycles and synoptic-scale variations," *J. Geophys. Res.* **105D**, 14531–14546 (2000).
11. K. P. Petrov, S. Waltman, E. J. Dlugokencky, M. Arbore, M. M. Fejer, F. K. Tittel, and L. W. Hollberg, "Precise measurement of methane in air using diode-pumped 3.4-μm difference-frequency generation in PPLN," *Appl. Phys. B* **64**, 567–572 (1997).
12. S. Waltman, K. P. Petrov, E. J. Dlugokencky, M. Arbore, M. M. Fejer, F. K. Tittel, and L. W. Hollberg, "Measurement of <sup>13</sup>CH<sub>4</sub>/<sup>12</sup>CH<sub>4</sub> ratios in air using diode-pumped 3.3 μm difference-frequency generation in PPLN," in *1997 Digest of the IEEE/LEOS Summer Topical Meetings* (IEEE Press, 1997), pp. 37–38.
13. T. B. Coplen, "Reporting of stable hydrogen, carbon, and oxygen isotopic abundances (technical report)," *Pure Appl. Chem.* **66**, 273–276 (1994).
14. D. Guenther, *Carbon Cycle Greenhouse Gases Group*, Earth System Research Laboratory, National Oceanic and Atmospheric Administration, Boulder, Colo. (personal communication, 2005).